Influence of the Bridge, Island Area, Bass Bar and Soundpost on the Acoustic Modes of the Violin.

Colin Gough

School of Physics and Astronomy, University of Birmingham, B15 2TT, UK
profgough@googlemail.com

ABSTRACT

The influence of the bridge, f-holes, island area, soundpost and bass bar on the vibro-acoustic modes of the violin has been investigated over a wide range of frequencies using COMSOL shell structure finite element (FEA) computations. The body shell modes other than in the island area have been strongly damped to reveal the smoothly varying frequency spectrum of the bridge-island area input filter controlling the energy transfer from the bowed string to the radiating shell modes. Of special relevance is the so-called *BH*-feature between around 2-3 kHz, often correlated with the quality of fine sounding violins.

1. INTRODUCTION

In a pair of related publications [1, 2], the violin was modeled as a thin-walled, guitar-shaped box, with arched top and back plates coupled around their edges by shallow ribs. COMSOL 3.5 finite element shell structure software was used as an aid to understanding the acoustically important signature modes below around 1 kHz and their relationship to the freely supported top and back plates before assembly. This paper extends the investigation to address the influence of the bridge, f-holes, the island area between them and the bass bar and offset soundpost on the vibro-acoustic modes of the violin up to 10 kHz. These components introduce an acoustic filter between the transverse bowed string forces at the top of the bridge and the major radiating surfaces of the body shell, hence quality of sound of an instrument.

Of particular interest is a rather broad peak in amplitudes of the excited plate resonances often observed in the range 2-3 kHz, referred to as the *BH* or bridge hill feature. This was originally associated with the in-plane mode of the top section of the bridge rocking about its waist originally identified by Reinicke [3] - typically at around 3 kHz, when mounted on a rigid base.

Dunnwald [4] and Jansson[5] both noted the appearance of such a feature in several classic Cremonese Italian violins. However, Bissinger [6], observed little evidence for any such correlation in measurements on 12 violins of widely varying quality.

Jansson and Niewczyk[7] also observed the *BH* hill feature on some instruments with a rigid bridge, with no rocking mode resonance in the frequency range of interest. They therefore concluded that it was not necessarily a property of the bridge alone. Subsequently, Durup and Jansson [8], using simplified inverted L-shaped "f-holes" cut into a rectangular flat plate, identified a strong correlation of the *BH* feature with a *flapping* resonance of the upper inner-corner "wings" of the island area. Jansson and co-researchers [9] have recently identified a similar mode from finite element computations for simply modeled f-holes cut into both flat and arched rectangular plates.

At high frequencies, there is a high density and large overlap of the damped resonances of the body shell. In such cases a statistical approach can be used to describe the frequency-averaged response of the plate modes, as described by Cremer [10], Chpt.11 and Woodhouse[11].

Woodhouse used a SEA (Statistical Energy Analysis) approach to derive "skeleton" curves describing the smoothly varying, mode-averaged, input filter response of a simply modeled bridge mounted on a rectangular plate. In this model, the bridge vibrations were strongly damped by the resistive, thin plate, point driving-impedance of the supporting plates, $Z_o = \frac{\sqrt{3}}{4} c_{gm} \rho h^2$, where $c_{gm}\rho$ is the geometric mean of the along- and cross-grain characteristic impedances of longitudinal waves and h is the plate thickness. The resulting losses significantly broaden the rocking mode resonance. In addition, the mutual plate deformations around the two feet of the bridge result in a filter response dependent on their separation.

As recognized by Woodhouse, the original model ignored the influence of the nearby free edges of the f-holes forming an island area with its own localised modes between them, though they were included for a parallel slit geometry in a later hybrid SEA + FEA MSc project by Smith[12].

Such complications are automatically taken into account in the present paper, which describes the use of finite element computations to investigate and understand the influence of the bridge and plate properties on the *BI*, bridge-island, input filter and the additional role played by the offset soundpost and bass bar. Hopefully, such understanding may provide a helpful guide to luthiers in making and setting up any instrument of the violin family to optimize its sound.

2. THE FINITE ELEMENT MODEL

The body shell geometry of the violin used in this paper is identical to that described earlier papers [1, 2], except that an island area is now defined between the upper and lower bout areas of the top plate, as illustrated in Fig.1. The bridge and island area are only weakly damped (η = 0.01), while the remaining areas of the top and back plates are strongly

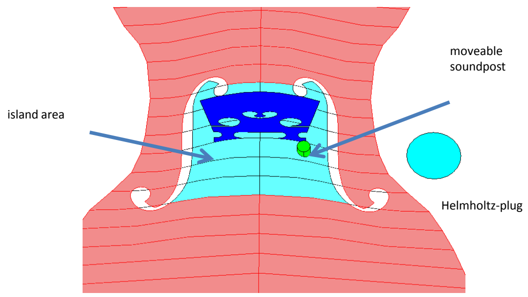

Figure 1. The division of the top plate into an island area separating the strongly damped lower and upper bout areas.

damped (η =1). The filter response of the bridge and island area can then be computed as a smoothly varying function of frequency uncomplicated by the multi-resonant response of the body shell vibrations, as illustrated in figure 2.

This is similar to Woodhouse's analytic "skeleton" curve model [11], but with the coupling to the vibrating plate modes now moved to the upper and lower boundaries of the island area, rather than under the two bridge feet. As the energy radiated from the ends of the island area rapidly decays to a small value at the plate edges, we have simply pinned the top plate edges. Coupling to the back plate modes is then only via the soundpost, when present.

Because the influence of the along- to cross-grain elastic anisotropy, $A = E_{along}/E_{cross}$, is important for the localised island area modes, the lengths of the top and back plates have been decreased by $A^{1/8}$ and widths increased by the same factor maintaining the same area and geometric mean $E_{gm} = \sqrt{E_{along}E_{cross}}$. At high frequencies, when arching is no longer important, the bending wave solutions of the transformed geometry then reproduce those of the unscaled anisotropic thin plates (Cremer [10]§11.2). For a spruce top plate with typical anisotropy of 20, a scaling factor of 1.45 has been used, and 1.22 for the maple back plate with typical anisotropy of around 5.

A bridge of mass 2.2 g has been used, with its thickness tapered from 4 mm at the bridge feet to 1.5 mm at the top. A density of 660 kgm^{-3} has been assumed with an isotropic Young's constant of 4e9 GPa giving a rocking frequency resonance of the top half of the bridge about the waist of 3.08 kHz, when mounted on a rigid base. To distinguish between the uncoupled bridge modes and those of the island area, additional computations were made with the rigidity of the bridge increased by a factor of 10^4, with its mass unchanged. This raises the rocking mode frequency far beyond any frequency of interest.

Initially, an unscaled, simply-shaped, bass bar was used of thickness 5 mm, maximum height 16 mm at its center and length 12.5 cm running lengthwise under the bass foot of the bridge. Exact dimensions are unimportant, as both the bridge and bass bar properties have been varied over several orders of magnitude to identify and understand their influence on the bridge-island filter action.

The body shell is excited by a 1N sinusoidal force at the top of the bridge in line with the bridge plane, either parallel $F_{\parallel}$ or perpendicular $F_{\perp}$ to the supporting ribs. The resulting amplitude and phase of the in-line velocity gives the input admittance A. For brevity, only $F_{\parallel}$ will be considered here with plots of the admittance in phase with the exciting force. This determines the rate of energy transfer from the vibrating strings to the acoustically radiating body shell modes, apart from small losses in the bridge and island area.

3. ISLAND AREA AND F-HOLES

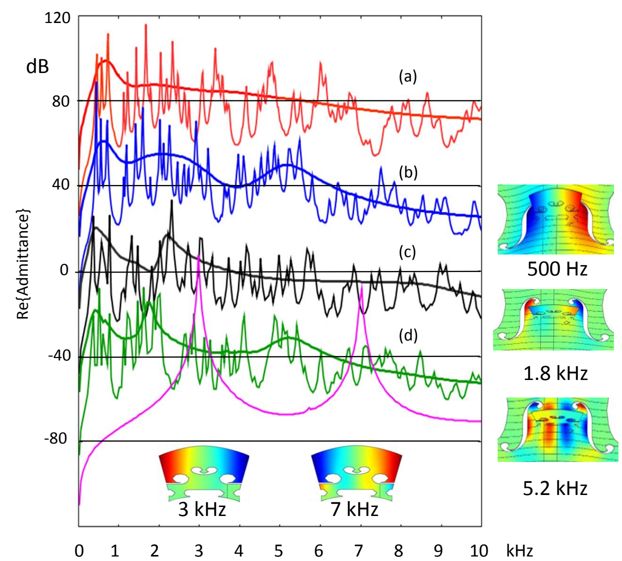

Figure 2. The computed in-line, in-phase, $F_{\parallel}$ admittance, for a rigid bridge mounted on the empty body shell, initially without bass bar or f-holes, with both lightly ($\eta = 0.01$) and heavily damped ($\eta = 1$) plate modes: (a) for a bridge with rigidity increased by 10^4 and (b) with normal rigidity. Then, after opening the f-holes, (c) with bridge rigidity increased by 10^4 and (d) for normal rigidity. The curves have been shifted by 20 dB to identify the separate characteristics. The mode shapes to the right of the plot are the dominant resonant island area modes, while those below are the in-plane resonances of the bridge resting on a rigid base including the rocking mode at 3 kHz.

Figure 2 illustrates how heavily damping the body shell modes reveals the underlying frequency dependent filtering of the bridge-island area. The measurements shown are for an isotropic top plate before the plates were scaled to account for anisotropy. The upper two sets of curves illustrate the admittances of the empty body shell before the f-holes are cut into the top plate. First in (a), for a rigid bridge with the relatively featureless admittance determined by the energy radiated from under the two feet towards the outer edges of the top plate and in (b), with a normal bridge resulting in the superposition of two rather broad resonances at a significantly lower frequency than those of the bridge alone mounted on a rigid base, which are also illustrated. The rigidly mounted bridge modes are the previously described rocking mode at ~ 3 kHz and a higher frequency mode at ~ 7 kHz involving bending of the lower areas of the bridge rotating in anti-phase with the top of the bridge.

The lower two curves illustrate the frequency dependence of the admittance at the top of the bridge with f-holes cut into the top plate. Figure (c) illustrates the admittance for a rigid bridge, with two strong broad resonances centered on ~ 500 and 1.8 kHz. These arise from the resonant excitation of the first two intrinsic island area modes illustrated to the right of the plot. The lowest frequency mode is a transverse standing wave across the width of the island area confined approximately to its length. This mode will couple to many anti-symmetric modes of the body shell at both low and high frequencies. The resonance at around 1.8 kHz is equivalent to that of the "flapping" inner-wing mode originally identified in highly simplified f-hole structures by Durup and Jansson[8].

Unsurprisingly, there is no evidence in any of these plots of a strongly peaked resonance at the "rocking" frequency of the rigidly supported bridge. This is because the resonance is spread out over a very wide range of frequencies by its damping and coupling to the plate modes. It is therefore important to understand the influence on the admittance as the coupling between the bridge and island area is varied.

4. BRIDGE-ISLAND COUPLING

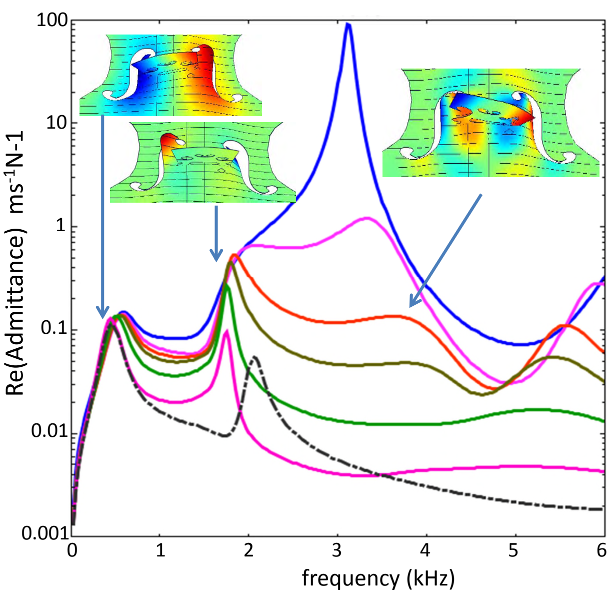

Figure 3. Dependence of the in-line, in-phase, $F_{\|}$ admittance of a tapered bridge of mass 2.2 g on the top plate island area of the body shell without bass bar or soundpost, as its mass and density are scaled by factors 0.01, 0.1, 0.3, 0.5, 1 and 2 from their unscaled value leaving the 3 kHz rigidly supported bridge rocking frequency unchanged. The bridge-island mode shapes are illustrated for frequencies just below their resonant peaks. The dash-dotted curve is for a rigid unscaled bridge mass with in-plane rocking frequency 100 times higher.

Consider first the in-line point admittance A_{input} at the top of the bridge, for a central driving force $F_{\perp}e^{i\omega t}$ exciting the *bouncing* mode of the bridge coupled to the localised symmetric modes of the island area. This can be written as

$$A_{input} = \frac{A_{island} + i\omega/m\omega_o^2}{[(1-\omega^2/\omega_o^2) + i\omega m A_{island}]}. \quad (1)$$

A_{island} is the effective admittance of the local island area modes under the two feet of the bridge, which are strongly damped by energy radiated into the upper and lower bouts of the top plate, while m is the effective mass of the *bouncing* mode of the rigidly supported bridge with $\omega_o = 2\pi f_{bouncing}$. An equivalent expression describes the admittance for $F_{\|}$, with appropriate A_{input}, m and *rocking* frequency.

The computed admittance is illustrated in Figure 3 for $F_{\|}$ exciting the heavily damped, anti-symmetric, body shell modes (without offset soundpost or bass bar), as the Young's modulus and density of the bridge are simultaneously scaled by the same wide-ranging factor, $bs = 0.01$ to 2, maintaining $f_{rocking}$ constant. The coupling of the bridge to the island area results in markedly different admittance curves from those for the bridge alone [11].

For the very light and flexible bridge (bs=0.01), the admittance at the top of the bridge is dominated by that of the bridge alone, with a strongly peaked resonance just above the rigidly supported bridge rocking frequency at 3.0 kHz. But as the admittance of the rocking bridge approaches that of the island area on which is stands, their modes of vibrations are strongly coupled together resulting in the illustrated veering and splitting of the resonant frequencies and damping of the *normal* modes describing their coupled vibrations.

The dash-dotted curve is for a rigid bridge of unscaled mass, but rocking frequency increased by a factor of 100. This illustrates the unperturbed resonances of the localized island area modes and the decrease in amplitude at higher frequencies from the inertial mass of the rocking bridge.

The lowest frequency peak in the admittance at ~ 400 Hz involves the initially rigid-body twisting vibrations of the island area coupled to the vibrations of the upper and lower bouts of the top plate. This transforms with increasing frequency into a strongly localized transverse bending mode of the island area. The strong, but relatively weakly damped resonance, just below 2 kHz involves the rigid body and rocking vibrations of the bridge vibrating in anti-phase with the "flapping" resonances inner wings of the island area, identified earlier by Durup and Jansson [8] for highly simplified f-hole shapes on a flat rectangular plate. The strongly damped resonance above the weakly coupled "rocking" 3 kHz frequency of the bridge rises to around 4 kHz, with the bridge now coupled to the next highest frequency transverse bending mode of the island area, with the top of the bridge now rocking in anti-phase with the top plate under its feet.

5. BASS BAR AND OFFSET SOUNDPOST

The addition of the bass bar and offset sound post has a very strong influence on the modes of the island area, hence cou-

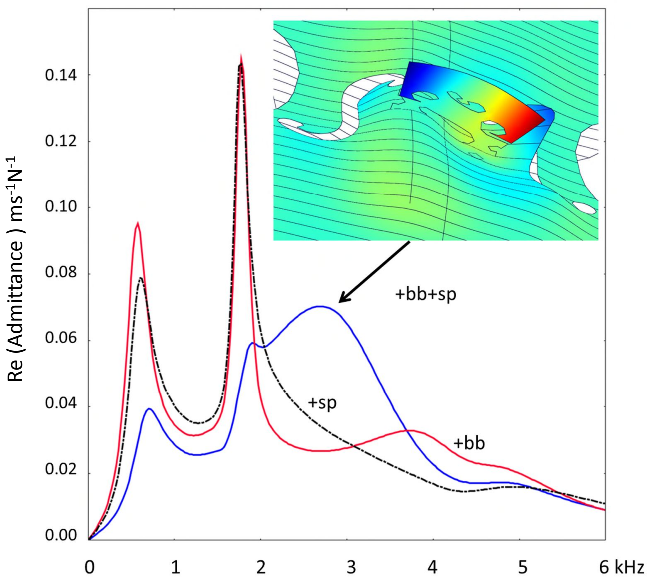

Figure 4. Influence of the bass bar and offset sound post on the BI admittance input filter (+bb+sp), the sound post alone (+sp) with bass bar removed and bass bar alone (+sb) with soundpost removed.

pling to the plate modes and sound of an instrument. Our model enables the contributions of the bass bar and offset soundpost to the overall filtering action of the bridge-island area to be investigated individually, as their coupling strengths are varied independently from zero to typical normal values. Likewise, the influence of arching, anisotropic Young's moduli, plate and bridge masses and rigidity can all be varied in a similar way - to be described in a more detailed account of the present investigation.

Here, we simply consider the influence of the bass bar and soundpost on the *BI* input filter, starting first with them both in place at full coupling strength and then removing them separately, to leave just the sound post or bass bar in place, as illustrated in figure 4. With both bass bar and soundpost in place, the computations reveal a pronounced *BI*-hill feature, with a very broad resonant response similar to the observed *BH* feature when present. The illustrated mode shape is clearly that of a very strongly damped normal mode, with the bridge rocking in anti-phase with the transverse vibrations of the island area. This clearly involves the inner-wings flapping resonance. However, the mode is slightly asymmetric, which is not surprising, as the bass bar and soundpost introduce asymmetry in opposite directions, which will only compensate for each other by accident.

In contrast, when only the bass bar or soundpost is present, the strong mid-frequency resonance disappears, with almost all the plate activity now concentrated in the region of the flapping inner-wing island area regions, with a top plate thickness dependence to be published later just below 2 kHz. Although the resonant frequencies are very similar, the modes are strongly asymmetric, with the vibrational amplitudes on the opposite side of the island always larger than close to the soundpost or bass bar, which tend to create nodal areas around or along them.

Figure 4 suggests that the input filter involving the localized vibrations of both the bridge and island area will strongly influence both the intensity and tonal balance of sound for all members of the violin family. This in turn will be strongly dependent on the offset soundpost and bass bar, "tuned" to balance the asymmetry induced in opposite directions. This explains why bass bar adjustments can play such a crucial role in the quality of sound of an instrument - as widely recognized by luthiers when setting up an instrument to optimize its sound.

Measurements are now required to test the predictions of the above model.

REFERENCES

[1] C. Gough, "Violin plate modes," *J. Acoust. Soc. Am.*, vol. 137, pp. 139–153, 2015.

[2] C. Gough, "A violin shell model:vibrational modes and acoustics," *J. Acoust. Soc. Am.*, vol. 137, pp. 1210–1225, 2015.

[3] W. Reinicke, "Die ubertrangungseigenschaften des streichinstrumentenstegs," 1973.

[4] E. Dunnwald, "Ein erweitertes vefahren zur objectiven bestimmung der klangqualitat von violinen," *Acustica*, vol. 71, pp. 269–276, 1990.

[5] E. Jansson, "Admittance measurements on 25 high quality violins," *Acta Acustica United with Acustica*, vol. 83, pp. 337–341, 1997.

[6] G. Bissinger, "The violin bridge as filter," *J. Acoust. Soc. Am.*, vol. 120, pp. 482–491, 2006.

[7] E. Jansson and B. Niewczyk, "On the acoustics of the volin: bridge or body hill?" *J. Catgut Acout. Soc. Series 2*, vol. 3, pp. 23–27, 1999.

[8] F. Durup and E. Jansson, "The quest of the violin bridge-hill," *Acta Acustica United with Acustica*, vol. 91, pp. 206–213, 2005.

[9] E. Jansson, R. Barczewski, and A. Kabala, "On the violin bridge hill- comparison of experimental testing and fem," *Vibrations in Physical Systems*, vol. 27, pp. 151–160, 2016.

[10] L. Cremer, "The physics of the violin," 1984.

[11] J. Woodhouse, "On the "bridge hill" of the violin," *Acta Acustica United with Acustica*, vol. 91, pp. 155–165, 2005.

[12] M. Smith, "Hybrid modelling of violin acoustics," Master's thesis, Engineering, Cambridge University, 2008.